TWO-TIME SCALE FORCE/POSITION CONTROL OF FLEXIBLE ROBOTS

PAOLO ROCCO

Dipartimento di Elettronica e Informazione
Politecnico di Milano
Piazza L. da Vinci, 32, 20133 Milano - Italy
rocco@elet.polimi.it

WAYNE J. BOOK

George W. Woodruff School of Mechanical Engineering
Georgia Institute of Technology
Atlanta, GA 30332-0405 - USA
wayne.book@me.gatech.edu

Abstract - **Distributed flexibility of the links is a severe obstacle for the endpoint position control of lightweight manipulators. In order to accomplish with satisfactory performance certain tasks involving a controlled interaction of the tip of the robot with the worksurfaces, a combined control of the motion and the contact forces can provide some advantages, as it is now recognized for rigid robots. This paper presents a model of a flexible robot interacting with a rigid environment, together with a control scheme designed to achieve the simultaneous control of both the motion of the end effector and the forces at the contact. The time scale separation of the control actions, deriving from singular perturbation theory, is exploited in the design of the controller, which is made up by modular and easy-to-tune components. Simulation results obtained on a detailed nonlinear model of an existing 2 d.o.f. flexible arm are also given.**

Keywords - **Flexible manipulators; force control; singular perturbation theory; composite control; robotic simulation.**

Submitted to the IEEE Transactions on Robotics and Automation - Regular Paper

1. INTRODUCTION

Lightweight flexible manipulators have lately earned increasing attention from robotic researchers. The demand for high speed and large workspace, coupled with the requirement of a high ratio between payload and arm masses, have stimulated engineers towards the investigation of new materials and mechanical designs, in an effort to overcome the limitations of rigid industrial robots. A variety of fields where the adoption of lightweight robots prove to be successful can now be characterized, including space robotics, exploration of hazardous environments and nuclear waste retrieval [1].

Distributed flexibility of the links, typical of lightweight structures, poses however some challenging problems, both from the modelling and the dynamic control standpoints. While for the dynamic modelling a somewhat satisfactory and widely adopted solution [2], [3] has been found, a number of solutions to the control problem have been and are still being proposed (see [4] for a recent comprehensive survey). As it is well known, much of the difficulty of the control problem stems from the nonminimum phase nature of the dynamic relation between the actuator torques at the joints and the endpoint position. Differently from the equations of the rigid robot and the (simplified) equations of the robot with joint flexibility [5], the input-state equations of the flexible robot are not feedback linearizable [6] while the input-output feedback linearization inevitably leads to unstable zero dynamics, which is the nonlinear counterpart of the nonminimum phase phenomenon.

Among the approximate solutions proposed to cope with these problems, the approach based on the separation of the control action into a slow and a fast component [7], [8] seems to be particularly promising. Singular perturbation theory [9], in fact, offers a powerful conceptual framework for an easy two-step design of the control system, based on an analogous two-step model of the system. As a remarkable feature, the controller for the "slow" system can be designed based on the rigid model of the system, which implies an inherent modularity of the overall control system, where the "fast" controller can be implemented or not depending on the desired performance and the available hardware.

However, even a satisfactory solution for the endpoint position control could prove to be inadequate for a successful fulfillment of certain tasks, requiring the interaction of the tip of the robot with the external environment. In these cases, it can be beneficial to monitor and control the forces and moments arising at the contact. The combined force/position control for rigid robots has been investigated since the early seventies and is still a very active area of research [10]. As far as the flexible manipulators are concerned, however, the literature is still at an early stage and only a few works dealing with this subject have been published so far.

The first attempts to investigate the nature of the control problem were conducted on the simplified linear model of a one-link flexible robot. Eppinger and Seering [11] and Li [12] emphasize the nonminimum phase nature of the noncolocated transfer function from the actuator torque to the force arising at the contact between the tip of the robot and the environment. The stability problem of a force controlled beam is also pointed out in [13] and [14], with reference to a reduced order linearized model of the robot.

A model for a 3 d.o.f. robot with tip reaction forces on a terminal flexible link is formulated in [15] and [16]. The control scheme is based on nonlinear feedback linearization with an additional term to stabilize the zero dynamics. Lew and Book [17] study the hybrid control of a flexible macro manipulator carrying a micro, in multiple contact with the environment for bracing. Experimental evidence of the feasibility of the control scheme is given. A similar scenario is considered in [18], but without a bracing strategy. The design of a hybrid control for a flexible arm is also the goal of [19]. Differently from the other works (where the assumed modes techniques is adopted), the authors develop the model of the flexible manipulator starting from first principles. Experimental results are offered which show acceptable tracking performances. In another work [20], which is perhaps the closest to the present one, Matsuno and Yamamoto develop a dynamic hybrid controller for a robot with a terminal flexible link. The authors propose a boundary condition which accounts for the presence of the constraint. Then they derive a singularly perturbed model, and design the slow controller as a hybrid controller. Singular perturbation theory was also used in [21], to prove that the application of a control law computed based on the rigid link equations of motion is still stable when applied to the flexible robots, provided that some conditions are satisfied, and in [22] to develop an adaptive hybrid position/force controller. In Section 3 we will point out some inconsistencies in these works dealing with the singular perturbation model of a constrained flexible robot. Finally, a robust controller based on Corless-Leitmann theory is proposed in [23].

The motivation of the present paper is twofold: on one hand, a rigorous model of a flexible robot constrained by a rigid environment is given, together with its singular perturbation version; on the other hand, a simple control strategy is proposed that achieves the simultaneous control of the motion and the contact force. While deriving from a detailed nonlinear model of the system and enjoying some strong theoretical properties, the proposed solution aims at being suitable for a straightforward implementation. A clear separation between the modules of the conventional position control, the additional fast control and the force control is respected, and each of these modules can be tuned independently of the others. Moreover, the transition between constrained and unconstrained motion is easily handled, since the position control is the same both in contact and in free motion, while the force controller automatically disconnects when the tip of the robot leaves the contact surface.

The paper is organized as follows: Section 2 develops the model of a constrained flexible robot, while Section 3 gives the singular perturbation version of the model; the two-time scale force/position controller is derived in Section 4, and is validated in Section 5 through simulations of a detailed dynamic model of the two d.o.f. flexible robot, RALF, built in the School of Mechanical Engineering of the Georgia Institute of Technology; finally some concluding remarks are proposed in Section 6.

2. MODEL OF A CONSTRAINED FLEXIBLE ROBOT

2.1 Model of the unconstrained flexible robot

Consider a n d.o.f. robotic arm whose links are affected by distributed elasticity. A finite dimensional model of the robot can be obtained by truncating the modal expansion of the deflection to a finite number of assumed modes [2], [3], under the assumption of small deformation:

$$w_i(x,t)=\sum_{j=1}^{m_i} q_{fij}(t)\psi_{ij}(x) \tag{1}$$

where w_i is the deflection of link i at time t, computed at a distance x from the origin of a suitable reference frame attached to the link, ψ_{ij} is the shape assumed for the j-th mode of link i, while q_{fij} is its time-varying amplitude. The number of modes retained from the asymptotic expansion is denoted by m_i.

Lagrange's equations of motion of the system can be obtained considering as a set of generalized coordinates, the rigid joint coordinates $q_r \in \Re^n$ and the flexible variables $q_f = (q_{f11}, \ldots, q_{f1m_1}; q_{f21}, \ldots, q_{f2m_2}; q_{fn1}, \ldots, q_{fnm_n})^T \in \Re^{N-n}$:

$$\boldsymbol{M}(\boldsymbol{q}_r,\boldsymbol{q}_f)\begin{bmatrix}\ddot{\boldsymbol{q}}_r\\ \ddot{\boldsymbol{q}}_f\end{bmatrix}+\begin{bmatrix}\boldsymbol{h}_r(\boldsymbol{q}_r,\dot{\boldsymbol{q}}_r,\boldsymbol{q}_f,\dot{\boldsymbol{q}}_f)\\ \boldsymbol{h}_f(\boldsymbol{q}_r,\dot{\boldsymbol{q}}_r,\boldsymbol{q}_f,\dot{\boldsymbol{q}}_f)\end{bmatrix}+\begin{bmatrix}\boldsymbol{g}_r(\boldsymbol{q}_r,\boldsymbol{q}_f)\\ \boldsymbol{g}_f(\boldsymbol{q}_r,\boldsymbol{q}_f)\end{bmatrix}+\begin{bmatrix}\boldsymbol{0}_{n,N-n}\\ \boldsymbol{K}\boldsymbol{q}_f\end{bmatrix}=\begin{bmatrix}\boldsymbol{B}_r^T(\boldsymbol{q}_r,\boldsymbol{q}_f)\\ \boldsymbol{B}_f^T(\boldsymbol{q}_r,\boldsymbol{q}_f)\end{bmatrix}\boldsymbol{u} \tag{2}$$

where:

$$M = \begin{bmatrix} M_{rr} & M_{rf} \\ M_{rf}^T & M_{ff} \end{bmatrix}$$

is the symmetric positive definite inertia matrix of the robot, conveniently partitioned into the matrices $M_{rr} \in \Re^{n\times n}$, $M_{rf} \in \Re^{n\times(N-n)}$, $M_{ff} \in \Re^{(N-n)\times(N-n)}$ and $M_{rf}^{\,T} \in \Re^{(N-n)\times n}$; h_r and h_f are the vectors of Coriolis and centrifugal terms, g_r and g_f are the vectors of gravitational terms (for the rigid and the flexible parts, respectively); K is the matrix (diagonal and definite positive) of the stiffness constants; $u \in \Re^n$ is the vector of the control inputs (assuming as many control inputs as rigid d.o.f.); B_r and B_f are the matrices that reflect the action of the control inputs u on the equations of the rigid and flexible variables, respectively. Notice that the expressions of matrices B_r and B_f depend on the boundary conditions adopted in the definitions of the mode functions: in case of clamped-free boundary conditions [2], with the links clamped to the actuators hubs, B_r is the identity matrix, while B_f is a null matrix; in case of pinned-pinned or pinned-free boundary conditions, B_f is a constant non null matrix. With complex transmission systems, both the matrices depend, in general, on the values of the rigid and flexible coordinates: Section 5 will present an example where this dependence is crucial in the mathematical model of the robot.

2.2 Constraints

Assume now that the tip of the robot makes contact with a very stiff environment. A convenient way to represent this situation is to write as many constraint equations as the number of d.o.f. inhibited by the interaction with the environment. The constraint equations are easily written in terms of the Cartesian coordinates of the tip of the robot, in a suitable reference frame. However, by way of the direct kinematics of the robot, we can always assume the constraint equations as written in terms of the above defined rigid joint coordinates q_r and flexible variables q_f:

$$\Phi(q_r, q_f) = \mathbf{0}, \tag{3}$$

where Φ: $(\Re^n \times \Re^{N-n}) \to \Re^m$, m being the number of constraints ($m \le n$).

Defining now the two Jacobian matrices:

$$A_r = \frac{\partial \Phi}{\partial q_r}, \qquad A_f = \frac{\partial \Phi}{\partial q_f},$$

where $A_r \in \Re^{m \times n}$, $A_f \in \Re^{m \times (N-n)}$, and recalling that the constraint forces act along the normals to the constraint surfaces, we can rewrite eq.(2), in case of constrained motion, as:

$$M(q_r, q_f)\begin{bmatrix} \ddot{q}_r \\ \ddot{q}_f \end{bmatrix} + \begin{bmatrix} h_r(q_r, \dot{q}_r, q_f, \dot{q}_f) \\ h_f(q_r, \dot{q}_r, q_f, \dot{q}_f) \end{bmatrix} + \begin{bmatrix} g_r(q_r, q_f) \\ g_f(q_r, q_f) \end{bmatrix} + \begin{bmatrix} \mathbf{0}_{n,N-n} \\ K q_f \end{bmatrix} = \begin{bmatrix} B_r^T(q_r, q_f) \\ B_f^T(q_r, q_f) \end{bmatrix} u + \begin{bmatrix} A_r^T(q_r, q_f) \\ A_f^T(q_r, q_f) \end{bmatrix} \lambda \tag{4}$$

where $\lambda \in \Re^m$ is a vector of Lagrange multipliers. It is possible [24], [25] to assign these multipliers a physical meaning in terms of the corresponding components of the reaction force and moment, by an appropriate choice of the Cartesian frame used to produce the constraint equations (3).

It is worth noting that the presence of the constraints does not involve any particular concern on the choice of the mode shapes ψ_{ij}, as long as an assumed modes technique is used. The assumed modes technique, in fact, requires that the mode functions satisfy the *geometric* boundary conditions, while *natural* boundary conditions (i.e. boundary conditions involving the balance of force and moments at the ends of the links) are automatically taken into account by the Lagrange formulation of the mathematical model [26]. Mode functions that also satisfy the natural boundary conditions, or a simplified version of them, could improve the accuracy of the model, but at the expense of a much more involved derivation of the mathematical model. Since the constraints on the motion of the tip of the arm do not alter the geometric boundary conditions, we will assume the same mode functions for the unconstrained dynamic model and the constrained one.

2.3 Model reduction

The mathematical model (4) is made up by N second-order differential equations, for a system that actually presents $N-m$ d.o.f., once the constraints (3) are active. It is however possible to reduce the number of differential equations, by resorting to a coordinate partitioning procedure [27], [28], [29]. Consider the following partition of the vector $\boldsymbol{q}_r$:

$$\boldsymbol{q}_r = \begin{bmatrix} \boldsymbol{q}_{r1} \\ \boldsymbol{q}_{r2} \end{bmatrix}, \tag{5}$$

where $\boldsymbol{q}_{r1} \in \Re^m$, $\boldsymbol{q}_{r2} \in \Re^{n-m}$, and assume that there exist a continuous, twice differentiable function Ω: $(\Theta_{r2}\times \Theta_f) \rightarrow \Re^m$, where Θ_{r2} and Θ_f are two open sets ($\Theta_{r2}\subset\Re^{n-m}$, $\Theta_f\subset\Re^{N-n}$), such that the constraints (3) can be expressed as:

$$\boldsymbol{q}_{r1} = \Omega(\boldsymbol{q}_{r2}, \boldsymbol{q}_f). \tag{6}$$

A reordering of the rigid variables $\boldsymbol{q}_r$ could be necessary to express the constraints as in (6). Also, note that the dependent variables $\boldsymbol{q}_{r1}$ have been chosen only among the rigid ones, thus implicitly excluding the presence of a constraint acting only on the flexible variables.

Differentiating (5) with respect to time, we have:

$$\dot{\boldsymbol{q}}_r = \boldsymbol{T}_{rr}\dot{\boldsymbol{q}}_{r2} + \boldsymbol{T}_{rf}\dot{\boldsymbol{q}}_f \tag{7}$$

where:

$$\boldsymbol{T}_{rr} = \begin{bmatrix} \dfrac{\partial\Omega}{\partial \boldsymbol{q}_{r2}} \\ \boldsymbol{I}_{n-m} \end{bmatrix} = \begin{bmatrix} -\boldsymbol{A}_{r1}^{-1}\boldsymbol{A}_{r2} \\ \boldsymbol{I}_{n-m} \end{bmatrix}, \quad \boldsymbol{T}_{rf} = \begin{bmatrix} \dfrac{\partial\Omega}{\partial \boldsymbol{q}_f} \\ \boldsymbol{0}_{n-m,N-n} \end{bmatrix} = \begin{bmatrix} -\boldsymbol{A}_{r1}^{-1}\boldsymbol{A}_f \\ \boldsymbol{0}_{n-m,N-n} \end{bmatrix}.$$

and the Jacobian matrix $\boldsymbol{A}_r$ has been partitioned as:

$$\boldsymbol{A}_r = \left[\boldsymbol{A}_{r1} \quad \boldsymbol{A}_{r2}\right] = \left[\frac{\partial \boldsymbol{\Phi}}{\partial \boldsymbol{q}_{r1}} \quad \frac{\partial \boldsymbol{\Phi}}{\partial \boldsymbol{q}_{r2}}\right],$$

where $\boldsymbol{A}_{r1} \in \Re^{m\times m}$, $\boldsymbol{A}_{r2} \in \Re^{m\times(n-m)}$, and $\boldsymbol{A}_{r1}$ is nonsingular.

Introducing matrix $\boldsymbol{T}$:

$$\boldsymbol{T} = \begin{bmatrix} \boldsymbol{T}_{rr} & \boldsymbol{T}_{rf} \\ \boldsymbol{0}_{N-n,n-m} & \boldsymbol{I}_{N-n} \end{bmatrix},$$

and noting that:

$$\left[\boldsymbol{A}_r \quad \boldsymbol{A}_f\right]\boldsymbol{T} \equiv \boldsymbol{0}\ , \tag{8}$$

it is possible to eliminate the Lagrange multipliers λ from the dynamic equations (4) by premultiplying the said equations by matrix $\boldsymbol{T}^T$. Exploiting the expression (7) and its derivative, we finally arrive at the expression of the constrained dynamic system in terms of the independent variables $\boldsymbol{q}_{r2}$ and $\boldsymbol{q}_f$:

$$\boldsymbol{M}_c(\boldsymbol{q}_{r2},\boldsymbol{q}_f)\begin{bmatrix}\ddot{\boldsymbol{q}}_{r2}\\ \ddot{\boldsymbol{q}}_f\end{bmatrix} + \begin{bmatrix}\boldsymbol{h}_{cr}(\boldsymbol{q}_{r2},\dot{\boldsymbol{q}}_{r2},\boldsymbol{q}_f,\dot{\boldsymbol{q}}_f)\\ \boldsymbol{h}_{cf}(\boldsymbol{q}_{r2},\dot{\boldsymbol{q}}_{r2},\boldsymbol{q}_f,\dot{\boldsymbol{q}}_f)\end{bmatrix} + \begin{bmatrix}\boldsymbol{g}_{cr}(\boldsymbol{q}_{r2},\boldsymbol{q}_f)\\ \boldsymbol{g}_{cf}(\boldsymbol{q}_{r2},\boldsymbol{q}_f)\end{bmatrix} + \begin{bmatrix}\boldsymbol{0}_{n-m,N-n}\\ \boldsymbol{K}\boldsymbol{q}_f\end{bmatrix} = \begin{bmatrix}\boldsymbol{B}_{cr}^T(\boldsymbol{q}_{r2},\boldsymbol{q}_f)\\ \boldsymbol{B}_{cf}^T(\boldsymbol{q}_{r2},\boldsymbol{q}_f)\end{bmatrix}\boldsymbol{u} \tag{9}$$

where:

$$\boldsymbol{M}_c = \begin{bmatrix}\boldsymbol{M}_{crr} & \boldsymbol{M}_{crf}\\ \boldsymbol{M}_{crf}^T & \boldsymbol{M}_{cff}\end{bmatrix}$$

and

$$\boldsymbol{M}_{crr} = \boldsymbol{T}_{rr}^T\boldsymbol{M}_{rr}\boldsymbol{T}_{rr},\quad \boldsymbol{M}_{crf} = \boldsymbol{T}_{rr}^T\boldsymbol{M}_{rr}\boldsymbol{T}_{rf} + \boldsymbol{T}_{rr}^T\boldsymbol{M}_{rf},\quad \boldsymbol{M}_{cff} = \boldsymbol{M}_{ff} + \boldsymbol{T}_{rf}^T\boldsymbol{M}_{rr}\boldsymbol{T}_{rf} + \boldsymbol{T}_{rf}^T\boldsymbol{M}_{rf} + \boldsymbol{M}_{rf}^T\boldsymbol{T}_{rf}\ ,$$

$$h_{cr} = T_{rr}^T h_r + T_{rr}^T M_{rr} \dot{T}_{rr} \dot{q}_{r2} + T_{rr}^T M_{rr} \dot{T}_{rf} \dot{q}_f, \quad h_{cf} = T_{rf}^T h_r + h_f + T_{rf}^T M_{rr} \dot{T}_{rr} \dot{q}_{r2} + M_{rf} \dot{T}_{rr} \dot{q}_{r2} + T_{rf}^T M_{rr} \dot{T}_{rf} \dot{q}_f$$

$$g_{cr} = T_{rr}^T g_r, \quad g_{cf} = T_{rf}^T g_r + g_f$$

$$B_{cr}^T = T_{rr}^T B_r^T, \quad B_{cf}^T = T_{rf}^T B_r^T + B_f^T \ .$$

An expression for the Lagrange multipliers λ in terms of the state variables can be obtained by twice differentiating the constraint equations (3) [29]:

$$A_r \ddot{q}_r + \dot{A}_r \dot{q}_r + A_f \ddot{q}_f + \dot{A}_f \dot{q}_f = \mathbf{0},$$

and eliminating the vector of the acceleration from eq. (4). The result is:

$$\lambda = \left(AM^{-1}A^T\right)^{-1}\left(-\dot{A}\begin{bmatrix} T_{rr}\dot{q}_{r2} + T_{rf}\dot{q}_f \\ \dot{q}_f \end{bmatrix} + AM^{-1}\left(\begin{bmatrix} h_r \\ h_f \end{bmatrix} + \begin{bmatrix} g_r \\ g_f \end{bmatrix} + \begin{bmatrix} \mathbf{0}_{n,N-n} \\ Kq_f \end{bmatrix} - \begin{bmatrix} B_r^T \\ B_f^T \end{bmatrix} u\right)\right), \quad (10)$$

where A=[A_r A_f].

As a result of the coordinate partitioning method, eq. (9) is formally identical to (2): this is in contrast with other reduction methods. In the SVD approach [17] the dynamic model would be expressed in terms of a position vector, combination of the rigid and flexible coordinates. Thus the separation between the rigid and the flexible dynamics, essential in the following developments, would be lost. Moreover, the SVD reduction can be consistently applied only when the constraints are linear or linearized around a reference position.

3. A SINGULARLY PERTURBED VERSION OF THE MODEL

A very reasonable way to approach the control problem of system (9) consists in separating the slow dynamics, associated with the rigid motion of the robot, from the fast dynamics related to the link flexibility. Singular perturbation theory [9] gives the tools to accomplish this task. Following [7], the first step consists in defining the singular perturbation parameter as $\mu = 1/k$, where k is a common factor among the stiffness constants of the arm (elements of matrix $\boldsymbol{K}$), say the smallest stiffness constants. New variables are then introduced as:

$$\zeta = \boldsymbol{K}\boldsymbol{q}_f = k\hat{\boldsymbol{K}}\boldsymbol{q}_f \ ,$$

with $\hat{\boldsymbol{K}} = 1/k\, \boldsymbol{K}$. Defining the inverse of the inertia matrix of the constrained system as:

$$\boldsymbol{H}_c = \boldsymbol{M}_c^{-1} = \begin{bmatrix} \boldsymbol{H}_{crr} & \boldsymbol{H}_{crf} \\ \boldsymbol{H}_{cfr} & \boldsymbol{H}_{cff} \end{bmatrix},$$

where $\boldsymbol{H}_{crr}$, $\boldsymbol{H}_{crf}$, $\boldsymbol{H}_{cff}$ and $\boldsymbol{H}_{cfr} = \boldsymbol{H}_{crf}^T$ have the same dimensions as $\boldsymbol{M}_{crr}$, $\boldsymbol{M}_{crf}$, $\boldsymbol{M}_{cff}$ and $\boldsymbol{M}_{crf}^T$ respectively, it is possible to rewrite system (9) in the following singularly perturbed form:

$$\ddot{\boldsymbol{q}}_{r2} = -\boldsymbol{H}_{crr}\left[\boldsymbol{h}_{cr} + \boldsymbol{g}_{cr}\right] - \boldsymbol{H}_{crf}\left[\boldsymbol{h}_{cf} + \boldsymbol{g}_{cf} + \zeta\right] + \left[\boldsymbol{H}_{crr}\boldsymbol{B}_{cr}^T + \boldsymbol{H}_{crf}\boldsymbol{B}_{cf}^T\right]\boldsymbol{u} \tag{11}$$

$$\mu\ddot{\zeta} = -\hat{\boldsymbol{H}}_{cfr}\left[\boldsymbol{h}_{cr} + \boldsymbol{g}_{cr}\right] - \hat{\boldsymbol{H}}_{cff}\left[\boldsymbol{h}_{cf} + \boldsymbol{g}_{cf} + \zeta\right] + \left[\hat{\boldsymbol{H}}_{cfr}\boldsymbol{B}_{cr}^T + \hat{\boldsymbol{H}}_{cff}\boldsymbol{B}_{cf}^T\right]\boldsymbol{u} \ , \tag{12}$$

being $\hat{\boldsymbol{H}}_{cfr} = \hat{\boldsymbol{K}}\boldsymbol{H}_{cfr}$ and $\hat{\boldsymbol{H}}_{cff} = \hat{\boldsymbol{K}}\boldsymbol{H}_{cff}$. Observe that in this paper the singularly perturbed model is derived based upon the reduced order model (9) of the constrained mechanical system, rather than on the original constrained model (4). This will lead to some interesting consequences in the following developments

In the limit as $\mu \rightarrow 0$, eq. (12) collapses to the following algebraic equation:

$$\begin{aligned} \bar{\zeta} = \hat{\boldsymbol{H}}_{cff}^{-1}(\bar{\boldsymbol{q}}_{r2},\boldsymbol{0})\Big[&-\hat{\boldsymbol{H}}_{cfr}(\bar{\boldsymbol{q}}_{r2},\boldsymbol{0})\left[\boldsymbol{h}_{cr}(\bar{\boldsymbol{q}}_{r2},\dot{\bar{\boldsymbol{q}}}_{r2},\boldsymbol{0},\boldsymbol{0}) + \boldsymbol{g}_{cr}(\bar{\boldsymbol{q}}_{r2},\boldsymbol{0})\right] + \hat{\boldsymbol{H}}_{cfr}(\bar{\boldsymbol{q}}_{r2},\boldsymbol{0})\boldsymbol{B}_{cr}^T(\bar{\boldsymbol{q}}_{r2},\boldsymbol{0})\bar{\boldsymbol{u}}\Big] \\ &-\boldsymbol{h}_{cf}(\bar{\boldsymbol{q}}_{r2},\dot{\bar{\boldsymbol{q}}}_{r2},\boldsymbol{0},\boldsymbol{0}) - \boldsymbol{g}_{cf}(\bar{\boldsymbol{q}}_{r2},\boldsymbol{0}) + \boldsymbol{B}_{cf}^T(\bar{\boldsymbol{q}}_{r2},\boldsymbol{0})\bar{\boldsymbol{u}} \end{aligned} \tag{13}$$

(the overbars denote that all the variables are evaluated in the special case μ=0). By plugging this equation into (11), with μ=0, the equations of the rigid robot model are obtained, as it can be proven: thus the slow dynamics of the system is readily identified as the dynamics of the rigid system.

To reveal the fast dynamics, we first introduce the so called fast variables:

$$\eta_1 = \zeta - \overline{\zeta}, \quad \eta_2 = \varepsilon\dot{\zeta}$$

where $\varepsilon = \sqrt{\mu}$, and then the fast time scale $\tau = t/\varepsilon$. Rewriting the system in this time scale, and examining it for ε=0, it is easy to conclude that system (11) confirms that $\boldsymbol{q}_{r2}$ and $\dot{\boldsymbol{q}}_{r2}$ are constant on the boundary layer, while the expression of the fast dynamics can be obtained by combining eq. (12) and eq. (13). The result is:

$$\begin{aligned} \frac{d\eta_1}{d\tau} &= \eta_2 \\ \frac{d\eta_2}{d\tau} &= -\hat{\boldsymbol{H}}_{cff}(\overline{\boldsymbol{q}}_{r2},0)\eta_1 + \left[\hat{\boldsymbol{H}}_{cfr}(\overline{\boldsymbol{q}}_{r2},0)\boldsymbol{B}_{cr}^T(\overline{\boldsymbol{q}}_{r2},0) + \hat{\boldsymbol{H}}_{cff}(\overline{\boldsymbol{q}}_{r2},0)\boldsymbol{B}_{cf}^T(\overline{\boldsymbol{q}}_{r2},0)\right](\boldsymbol{u}-\overline{\boldsymbol{u}}) \end{aligned} \qquad (14)$$

The expression (14) found for the fast dynamic system differs from the corresponding expression for the unconstrained flexible robot, as reported in (Siciliano and Book, 1988), where $\boldsymbol{B}_r = \boldsymbol{I}$ and $\boldsymbol{B}_f = \boldsymbol{0}$. Note, in fact, that all the matrices appearing in (14) depend on the constraint equations through the relations worked out in the previous Section. In other works dealing with singularly perturbed models of constrained flexible robots, such as [20], [21], [22], the same expression is found for constrained as for unconstrained motion. This is due to the fact that in these works, the singularly perturbed model is derived directly from the constrained equations (2), still containing the Lagrange multipliers. However, when computing the fast dynamic system, the fact that the Lagrange multipliers depend on both the slow and the flexible variables, as it is apparent from eq. (10), is ignored. Taking into account this essential fact, an additional term, related to difference between the expression of λ

computed at a generic ζ and the expression of λ computed at $\zeta = \overline{\zeta}$, would appear, which, in turn, would lead to the expression (14). However, the same expression can be derived in a much more straightforward way as shown above, i.e. by first deriving the motion equations of the constrained system in the residual d.o.f. and then applying the singular perturbation decomposition.

4. A TWO-TIME SCALE FORCE/POSITION CONTROLLER

4.1 Composite control

The separation between the slow (rigid) system and the fast system suggests a similar separation in the control action. The composite control strategy actually pursues this goal by splitting the control action as:

$$\boldsymbol{u} = \overline{\boldsymbol{u}}\left(\overline{\boldsymbol{q}}_{r2}, \dot{\overline{\boldsymbol{q}}}_{r2}\right) + \boldsymbol{u}_f\left(\overline{\boldsymbol{q}}_{r2}, \eta_1, \eta_2\right),$$

with $\boldsymbol{u}_f\left(\overline{\boldsymbol{q}}_{r2}, \boldsymbol{0}, \boldsymbol{0}\right) = \boldsymbol{0}$. The signal $\overline{\boldsymbol{u}}$ is responsible for the control of the slow subsystem, while the remaining part of the control vector, $\boldsymbol{u}_f$, is designed to control the fast system dynamics, while being inactive along the solutions of the slow subsystem.

If $\boldsymbol{u}_f$ uniformly stabilizes the fast system (14) around the equilibrium trajectory (13), it is possible to prove [9] that the following approximations hold (Tikhonov's theorem):

$$\boldsymbol{q}_{r2} = \overline{\boldsymbol{q}}_{r2} + O(\varepsilon), \quad \dot{\boldsymbol{q}}_{r2} = \dot{\overline{\boldsymbol{q}}}_{r2} + O(\varepsilon)$$

$$\zeta = \overline{\zeta} + \eta_1 + O(\varepsilon), \quad \varepsilon\dot{\zeta} = \eta_2 + O(\varepsilon),$$

where η_1 and η_2 are the solutions of system (14).

In other words, the solutions of the system differ from the solutions of the rigid system by an error whose order of magnitude is ε, for ε sufficiently small.

4.2 Design of the slow control system

The goal of the slow control action $\overline{u}$ is to make the tip of the robot track a prescribed trajectory while maintaining a desired force contact with the environment. As already said, the controller is designed based on the model of the rigid robot.

Instead of adopting a complete hybrid control strategy [28], [19], we adopt here a much more application oriented solution, similar to the one already proposed in [24], [31]. A distinctive feature of this solution is that the position control scheme remains the same both in unconstrained and constrained motion, while the force control closes an outer loop around the position control loops in constrained tasks, while being idle in unconstrained motion.

To be more specific, let us rewrite the model of the constrained rigid robot as:

$$\overline{M}_{crr}(\overline{q}_{r2})\ddot{\overline{q}}_{r2} + \overline{h}_{cr}(\overline{q}_{r2},\dot{\overline{q}}_{r2}) + \overline{g}_{cr}(\overline{q}_{r2}) = \overline{T}_{rr}^{T}(\overline{q}_{r2})\overline{\tau} \tag{15}$$

where $\overline{M}_{crr}(\overline{q}_{r2}) = M_{crr}(\overline{q}_{r2},0)$, $\overline{h}_{cr}(\overline{q}_{r2},\dot{\overline{q}}_{r2}) = h_{cr}(\overline{q}_{r2},\dot{\overline{q}}_{r2},0,0)$, $\overline{g}_{cr}(\overline{q}_{r2}) = g_{cr}(\overline{q}_{r2},0)$ and $\overline{T}(\overline{q}_{r2}) = T(\overline{q}_{r2},0)$, while $\overline{\tau} = B_r^T(\overline{q}_{r2},0)\overline{u}$ is the torque control input equivalent to the actual control input $\overline{u}$.

The position controller is designed with reference to the unconstrained model, as a decentralized PD controller plus a gravity compensation term:

$$\overline{\tau} = K_P(q_{dr} - \overline{q}_r) + K_D(\dot{q}_{dr} - \dot{\overline{q}}_r) + \overline{g}_r(\overline{q}_r) \tag{16}$$

where K_P=diag$\{K_{Pi}, i=1,...,n\}$, K_D=diag$\{K_{Di}, i=1,...,n\}$ are the matrices of the proportional and derivative gains of the PD controllers, respectively, $q_{dr} \in \Re^n$ is the vector of the position setpoints, while $\overline{g}_r(\overline{q}_r) = g_r(\overline{q}_r,0)$. It is well-known [32] that such a control strategy applied to a rigid robot ensures the global asymptotic stability of the equilibrium point resulting from the application of constant setpoints.

Consider now the vector of the setpoint q_{dr} as split into two components:

$$q_{dr} = q_{dr}^{M} + q_{dr}^{F}\ , \tag{17}$$

where q_{dr}^{M} is the motion setpoint, while q_{dr}^{F} is an additional term added to control the interaction force in case of constrained motion ($q_{dr}^{F} = \mathbf{0}$ in the unconstrained motion). The motion setpoint q_{dr}^{M} will be determined by way of the kinematic inversion of a suitable reference trajectory for the tip of the tool. We will assume in the sequel that, in case of constrained motion, the position setpoints satisfy the constraint equations. In other words:

$$\Phi\left(q_{dr}^{M}, \mathbf{0}\right) = \mathbf{0}\,. \tag{18}$$

The force control action, exerted through the additional position setpoints q_{dr}^{F}, will be designed so as to be active along the directions constrained by the environment, without affecting the motion control. Moreover, we will specify a zero steady state error between the setpoints λ_d and the Lagrange multipliers $\overline{\lambda}$. All the above requirements are satisfied if the force controller is designed based on the following relations:

$$K_P q_{dr}^{F} + K_D \dot{q}_{dr}^{F} = v^{F} \tag{19}$$

$$v^{F} = \overline{A}_r^{T}\left(\overline{q}_r\right) u^{F} \tag{20}$$

$$u^{F} = K_I^{F} \int \left(\lambda_d - \overline{\lambda}\right) dt \tag{21}$$

where $K_I^{F} = \mathrm{diag}\{\, K_{Ii}^{F},\, i=1,\ldots,m\}$.

Eq. (19) states that the additional position setpoints q_{dr}^{F} are obtained by filtering a suitable signal $v^F \in \Re^n$ through a decoupled dynamic system whose transfer function matrix is the inverse of the transfer function matrix of the PD regulators (refer to Fig. 1). Vector v^F, in turn, depends (20) on a m-dimensional vector $\boldsymbol{u}^F$ by way of the transpose of the Jacobian of the constraint equations: thus, whatever the value assumed by $\boldsymbol{u}^F$, $\boldsymbol{v}^F$ will be always oriented along the constrained directions. Finally, the control variable $\boldsymbol{u}^F$ is obtained as a decoupled integrator of the errors on each component of the Lagrange multipliers vector.

The following theorem establishes the theoretical properties of the proposed solution:

Theorem 5.1

The equilibrium point of the constrained system (15), controlled through (17), (19), (20), (21), under the assumption (18), corresponding to constant setpoints $\boldsymbol{q}_{dr}^M(t) = \tilde{\boldsymbol{q}}_{dr}^M$, $\lambda_d(t) = \tilde{\lambda}_d$, is globally asymptotically stable for every positive value of K_{pi}, K_{di} (i=1,...,n) and K_{Ii}^F (i=1,...,m).

Moreover, the equilibrium point is characterized by zero error for both the position and the force controllers: $\bar{\boldsymbol{q}}_r(t) = \tilde{\boldsymbol{q}}_{dr}^M$, $\bar{\lambda}(t) = \tilde{\lambda}_d$.

Proof:

See Appendix. ■

Remark

It is worth noting that the same positional control law (16) leads to a globally asymptotically stable equilibrium point both in case of unconstrained motion and in case of constrained motion. This is in contrast with other positional control law designed for the unconstrained robot, such as the computed torque. The force-position control scheme exploits the above property by making the position control loops independent of the force control loop, from a stability standpoint. Moreover, the stability analysis of the force control loop is trivial, since it reduces to the stability of a linear first order system.

Remark

From the above equations it is easy to conclude that $\overline{\lambda}$ is given by:

$$\overline{\lambda} = -\boldsymbol{u}^F + \gamma\left(\overline{\boldsymbol{q}}_{r2}, \dot{\overline{\boldsymbol{q}}}_{r2}, \boldsymbol{q}_{dr}^M\right) , \tag{22}$$

where γ is a complex term (see eq. (A.3) in the appendix), independent of $\boldsymbol{u}^F$. Thus the relation between the controller outputs $\boldsymbol{u}^F$ and the controlled variables $\overline{\lambda}$ amounts just to an algebraic system, which makes the tuning of the integral gains $\boldsymbol{K}_I^F$ straightforward.

4.3 Design of the fast control system

The fast controller must be designed so as to stabilize the fast system dynamics expressed by (14). A reasonable way to achieve this goal is to design a state-space control law as:

$$\boldsymbol{u}_f(\overline{\boldsymbol{q}}_{r2}, \eta_1, \eta_2) = \boldsymbol{K}_1(\overline{\boldsymbol{q}}_{r2})\eta_1 + \boldsymbol{K}_2(\overline{\boldsymbol{q}}_{r2})\eta_2 . \tag{23}$$

In principle, the feedback matrices $\boldsymbol{K}_1$ and $\boldsymbol{K}_2$ should be tuned for every configuration $\overline{\boldsymbol{q}}_{r2}$ to guarantee the best closed-loop performances. However, the computation burden necessary to perform this strategy can be avoided [7] by tuning the two matrices with reference to a given configuration and using the same matrices throughout the whole task, provided that the closed loop fast system will not go unstable along the slow trajectory. A numerical analysis of the eigenvalues of the closed loop system at varying $\overline{\boldsymbol{q}}_{r2}$, possibly throughout the entire workspace of the robot, should then accompany the synthesis made with reference to a specific configuration.

As far as the algorithm used to design the feedback control is concerned, any state-space technique can be used that achieves stability of the closed loop. In particular, since the location of the closed-loop eigenvalues assumes a crucial importance for the success of the singular perturbation control, a pole-placement algorithm can be used.

Remark

Numerical differentiations or dynamic observers [8] could be necessary to obtain estimates for the derivatives $\dot{q}_f$ of the flexible coordinates, whose measures are not usually available.

Remark

The control law (23) actually requires measures of the fast variables η_1, defined as the difference between the flexible forces ζ and the value $\overline{\zeta}$ assumed by these flexible forces along the slow trajectory. The expression (13) for $\overline{\zeta}$ is however quite complicated and can hardly be computed online. A practical way to cope with this problem is to obtain an approximation for $\overline{\zeta}$ by low pass filtering the measures of ζ, at a frequency equal to the crossover frequency of the slow controller, so as to guarantee that the fast controller is inactive along the solutions of the slow system.

4.4 Overall controller

The overall controller is obtained as:

$$\boldsymbol{u} = \left[\overline{\boldsymbol{B}}_r^T(\overline{\boldsymbol{q}}_{r2})\right]^{-1} \overline{\tau}\left(\overline{\boldsymbol{q}}_{r2}, \dot{\overline{\boldsymbol{q}}}_{r2}\right) + \boldsymbol{u}_f\left(\overline{\boldsymbol{q}}_{r2}, \eta_1, \eta_2\right) ,$$

where $\overline{\tau}$ is given by (16), with (17), (19), (20), (21), while u_f is given by (23).

5. SIMULATION RESULTS

The robot modelled in the simulations is RALF (Robotic Arm Large and Flexible), an experimental arm designed and built at the School of Mechanical Engineering of Georgia

Tech. Among the distinctive features of RALF (Fig. 2), it is worth recalling the large workspace, allowed by the two very long (about 3 *m* each) links, the hydraulic actuators and the parallelogram mechanism used to actuate the second link. Table 1 summarizes the physical parameters used in the simulation of RALF.

	Link 1	Link 2
Length (m)	3.048	3.048
Cross sectional area (m^2)	$2.773\ 10^{-3}$	$2.041\ 10^{-3}$
Density (Kg/m^3)	2707.	2707.
Young's module (N/m^2)	$7.1\ 10^{10}$	$7.1\ 10^{10}$
Area moment of inertia (m^4)	$6.308\ 10^{-6}$	$3.002\ 10^{-6}$

Table 1: RALF parameters

Two modes for each link are used to model the flexibility of the arm. Pinned-pinned boundary conditions [33] are considered adopting as trial functions the eigenfunctions of the associated single link problems:

$$\psi_{ij}(x) = \sin\left(\frac{j\pi x}{L_i}\right),$$

where L_i is the length of each link. The main reason for using pinned-pinned boundary conditions is that both the kinematic and the dynamic model of the arm are simpler than with other choices. In particular, the tip position depends only on the joint coordinates and not on the flexible variables, which simplifies the expression of the constraint, in case of contact with the environment. On the other hand, the control vector $\boldsymbol{u}$, see eq. (2), directly affects all the equations of motion, through matrices $\boldsymbol{B}_r$ and $\boldsymbol{B}_f$, while with clamped-free boundary conditions, for example, matrix $\boldsymbol{B}_f$ is null, provided that the actuator torques act along the rigid joint coordinates.

Notice, however, that in RALF the control vector $\boldsymbol{u}$ consists in the forces exerted by the hydraulic actuators, which obviously do not act along any joint coordinates. As a consequence, matrices $\boldsymbol{B}_r$ and $\boldsymbol{B}_f$ are full, whatever boundary conditions are chosen for the flexible modes and, in addition, they depend on both the joint and the flexible variables. A possible way to derive this dependence is to first compute the kinematic relation between the actuator lengths and the joint and flexible variables, and then derive $\boldsymbol{B}_r$ and $\boldsymbol{B}_f$ as the Jacobians of this relation with respect to the rigid and flexible variables, respectively. This is done in the model of RALF, and the said kinematic relation is found adopting some simplifying assumptions on the transmission mechanism of the second link.

Fig. 3 reports the Simulink© layout of the simulation plant. The numerical simulations have been performed with the Runge-Kutta 5th order integrator provided by Simulink. The equations of motion of the constrained system have been directly simulated, by solving the constraint with respect to one joint variable.

The robot is considered in contact with a rigid vertical surface, orthogonal to the plane of the robot links. The contact point is ($x = -3.6\ m$; $y = 2.5\ m$), (x, y) being a coordinate system in the plane defined by the two links, with origin located at joint 1 and the y axis vertical. In this configuration, the fast system presents four pairs of imaginary eigenvalues at frequencies 288 *rad/s*, 327 *rad/s*, 1070 *rad/s* and 1089 *rad/s* (no damping is introduced in the robot model). These values have been checked by comparison with experimental results.

The time scale separation between slow and fast dynamics has to be respected also in closed loop. To this aim, the PD gains of the slow controller are tuned in such a way that the position loops are nominally second order systems with resonant frequency set to 30 *rad/s* and damping factor set to 0.6. The force controller compensates for the presence of the PD controllers and closes its loop with the integral gain set to $K_I^F = 30$. Based on eq. (22), this value ensures a nominal crossover frequency of the force control loop equal to 30 *rad/s*. The fast system eigenvalues are left at the same natural frequencies as in open loop, but with damping factor set to 0.6. Matrices $\boldsymbol{K}_1$ and $\boldsymbol{K}_2$ are computed as the result of the multi input pole placement problem solved in the MATLAB Control System Toolbox [34]. A numerical analysis has been performed to check the positions of the eigenvalues when the rigid coordinates move from the reference position. The entire workspace of the robot has been explored, both on the constraint and in free motion. Fig. 4 reports the maximum real part of the eigenvalues of the closed loop system matrix with respect to the rigid coordinates, the surface being the result in the free space, the line the same quantity evaluated on the constraint. Notice that the expression of the dynamics of the fast system (and hence the eigenvalues) differs in the constrained motion from the unconstrained motion. Since the real part of the eigenvalues is always negative (actually less than -0.15), it is possible to conclude that the closed loop fast system is stable whatever the values of the slow coordinates, so that Tikhonov's theorem can be applied.

In a first set of simulations, the robot is initially at rest, in contact with the external surface, with the force control loop open. The initial value of the force is determined by the values assumed by the state variables at this equilibrium point. At time t=0, the force control loop is closed, with the force setpoint set to 50 N. Fig. 5 shows the force response with both the slow and the fast control closed, while in the simulation of Fig.6 the fast control has been left open: both the stable response of Fig. 5 (with the initial nonminimum phase inverse response) and the unstable response of Fig. 6 are consistent with the theory.

In a second set of simulations, the robot moves while in contact with the surface, with the force setpoint kept at the initial value. The commanded trajectory is a vertical downward segment, 0.2 m long, with a symmetric trapezoidal velocity profile: the maximum velocity is 0.15 m/s, while the acceleration in the initial and final parts is 0.2 m/s^2. Fig. 7 shows the force history during the trajectory tracking. The force controller keeps the error under ±0.5 N, and the recovery from the errors due to the discontinuities in the acceleration profile looks acceptable. Finally, Fig. 8 shows the trajectory tracking error, computed as the difference between the commanded and the simulated Cartesian positions along the vertical directions (the horizontal one being constrained). The steady-state error is due to the imperfect compensation of the steady state gravitational disturbance caused by the arm flexibility and is kept in an acceptable range (less than 0.4 *mm*).

6. CONCLUSIONS

The force/position control problem for flexible manipulators has been addressed and extensively discussed in this paper. The model reduction obtained via coordinate partitioning has allowed the derivation of a general formulation of the dynamic equations for a constrained flexible manipulator, which had not yet been presented in the literature. Moreover, a correct formulation of the singularly perturbed version of the model, whose fast subsystem has a different expression than in unconstrained motion, has been presented.

A conceptually simple control scheme has been also proposed, whose features are here briefly summarized.

Achievement of the control goals: the control goal was the simultaneous control of both the tip positions and the force arising at the interaction with the environment. This goal is achieved with zero steady-state error on the force and negligible steady-state error on the position. Moreover the fast dynamics related to the flexibility of the links is stabilized and damped.

Theoretical properties: the system ensures that the equilibrium point of the slow (rigid) system is globally asymptotically stable, while the trajectories of the fast subsystem converge towards the trajectories imposed by the slow system.

Modularity: the control scheme is made up by separate blocks that can be implemented or not depending on the available control architecture (hw/sw): the base controller is a positional decoupled PD on the joint angles; then a gravity compensation can be added to ensure a zero steady state error for the rigid system; a state space feedback on the flexible variables is then added to damp the fast dynamics; finally, an outer force control loop can be closed to ensure the control of the interaction force. Note that the addition of a module does not involve any change in the tuning of the other modules.

Easy design of the 'slow' controller: the position controller (PD+gravity compensation) is the same both in unconstrained and constrained motion. There is no need to define a partition of the joint coordinates in the control algorithm. The force control acts as an outer loop and can be automatically excluded in case of transition from constrained to unconstrained motion, by simply monitoring the measures of the force sensor.

Simulation results have proven the validity of the approach, while future experimental work on the same robot (RALF) used in the simulations will prove the actual feasibility of the ideas expressed in the present paper.

APPENDIX

Proof of theorem 5.1

Based on (16), (17), (19) and (20), the control torque τ can be expressed as[1]:

$$\tau = \boldsymbol{K}_P\left(\boldsymbol{q}_{dr}^M - \boldsymbol{q}_r\right) + \boldsymbol{K}_D\left(\dot{\boldsymbol{q}}_{dr}^M - \dot{\boldsymbol{q}}_r\right) + \boldsymbol{g}_r(\boldsymbol{q}_r) + \boldsymbol{A}_r^T(\boldsymbol{q}_r)\boldsymbol{u}^F \ .$$

Plugging the above expression into (15) and (10) and using (21), we obtain the closed loop dynamic equations of the system:

$$\boldsymbol{M}_{crr}(\boldsymbol{q}_{r2})\ddot{\boldsymbol{q}}_{r2} + \boldsymbol{h}_{cr}(\boldsymbol{q}_{r2},\dot{\boldsymbol{q}}_{r2}) = \boldsymbol{T}_{rr}^T(\boldsymbol{q}_{r2})\left[\boldsymbol{K}_P\left(\boldsymbol{q}_{dr}^M - \boldsymbol{q}_r\right) + \boldsymbol{K}_D\left(\dot{\boldsymbol{q}}_{dr}^M - \boldsymbol{T}(\boldsymbol{q}_{r2})\dot{\boldsymbol{q}}_{r2}\right)\right] \ , \qquad \text{(A.1)}$$

---

[1] To keep the notation simple, in the sequel we will drop the overbars on the variables, inessential for the proof.

$$\dot{x}^F = -K_I^F x^F + \gamma\left(q_{r2}, \dot{q}_{r2}, q_{dr}^M\right) - \lambda_d \tag{A.2}$$

where $q_r = \left[\Omega_r^T(q_{r2}, \mathbf{0}), q_{r2}^T\right]^T$, $x^F \in \Re^m$, while:

$$\gamma\left(q_{r2}, \dot{q}_{r2}, q_{dr}^M\right) = \left[A(q_r) M_{rr}^{-1}(q_r) A^T(q_r)\right]^{-1}$$
$$\left(-\dot{A}(q_r) T_{rr}(q_{r2}) \dot{q}_{r2} + A(q_r) M(q_r)^{-1}\left(h_r(q_r, \dot{q}_r) - K_P\left(q_{dr}^M - q_r\right) - K_D\left(\dot{q}_{dr}^M - T(q_{r2})\dot{q}_{r2}\right)\right)\right) \tag{A.3}$$

Notice that both in the dynamic equation (A.1) and in eq. (A.3) the gravity term has been compensated (perfect compensation is assumed), while in eq. (A.1) the force control term does not appear, since $T_{rr}^T(q_{r2}) A_r^T(q_r) = \mathbf{0}$ from (8). This is consistent with the requirement that the force control action act along the constrained directions, while not interfering with the motion control system.

Assume now that the system is subject to constant set-points $q_{dr}^M(t) = \tilde{q}_{dr}^M$, $\lambda_d(t) = \tilde{\lambda}_d$. Under the assumption (18) it will be possible to express the motion setpoints as $\tilde{q}_{dr}^M = \left[\Omega_r^T(\tilde{q}_{dr2}^M, \mathbf{0}), \tilde{q}_{dr2}^M\right]^T$, where $\tilde{q}_{dr2}^M \in \Re^{n-m}$. With this is mind, it is straightforward to conclude that the equilibrium point for the system (A.1), (A.2) is given by $q_{r2} = \tilde{q}_{dr2}^M$, $\dot{q}_{r2} = \mathbf{0}$, $x^F = -\left(K_I^F\right)^{-1} \tilde{\lambda}_d$. From (22) we also have $\lambda = \tilde{\lambda}_d$ at the equilibrium point.

Defining now the error variables:

$$e_{r2} = \tilde{q}_{dr2}^M - q_{r2}, \quad \dot{e}_{r2} = -\dot{q}_{r2} \ ,$$

we can rewrite, with some abuse of notation, system (A.1), (A.2) as:

$$M_{crr}(e_{r2})\ddot{e}_{r2} + h_{cr}(e_{r2}, \dot{e}_{r2}) + T_{rr}^T(e_{r2}) K_P e_r + T_{rr}^T(e_{r2}) K_D T_{rr}(e_{r2})\dot{e}_{r2} = \mathbf{0} \ , \tag{A.4}$$

$$\dot{x}^F + K_I^F x^F = \gamma\left(e_{r2}, \dot{e}_{r2}, q_{dr}^M\right) - \lambda_d \tag{A.5}$$

where $e_r = \tilde{q}_{dr}^M - q_r$. Observe that the system is made up by an autonomous part (A.4) having as state variables e_{r2} and $\dot{e}_{r2}$ and a second system (A.5), whose state variables are x^F, which is influenced by the first one through the function γ. As a consequence, the stability of the overall system is determined by the stability of the two subsystem separately. Moreover, (A.5) is a linear dynamic system, which is asymptotically stable for every positive definite K_I^F. To prove the global asymptotic stability of the equilibrium point, it is thus sufficient to prove the global asymptotic stability of the equilibrium point of system (A.4) (the origin of the state space). This can be done using the following Lyapunov function:

$$V = \frac{1}{2}\dot{e}_{r2}^T M_{crr}(e_r)\dot{e}_{r2} + \frac{1}{2}e_r^T K_P e_r \ , \tag{A.6}$$

which is positive definite for every positive definite K_P, since the constrained inertia matrix $\overline{M}_{crr}$ is positive definite everywhere. Differentiating V along the solution of the system, we obtain:

$$\dot{V} = \dot{e}_{r2}^T\left[\frac{1}{2}\dot{M}_{crr}(e_r)\dot{e}_{r2} - h_{cr}(e_{r2},\dot{e}_{r2}) - T_{rr}^T(e_{r2})K_D T_{rr}(e_{r2})\dot{e}_{r2} - T_{rr}^T(e_{r2})K_P e_r\right] + \dot{e}_r^T K_P e_r \ .$$

However, since $\dot{e}_r = T_{rr}(e_{r2})\dot{e}_{r2}$, the two terms in K_P cancel. Moreover, it is straightforward to verify that $1/2\,\dot{M}_{crr}(e_r)\dot{e}_{r2} - h_{cr}(e_{r2},\dot{e}_{r2}) = \mathbf{0}$, based on the analogous relation valid for the unconstrained model [35], so that:

$$\dot{V} = -\dot{e}_{r2}^T T_{rr}^T(e_{r2})K_D T_{rr}(e_{r2})\dot{e}_{r2} \ .$$

Thus $\dot{V} < 0,\ \forall \dot{e}_{r2} \neq \mathbf{0}$. Since, from (A.5), $\dot{e}_{r2} = \mathbf{0}$ implies $e_{r2} = \mathbf{0}$, LaSalle's theorem allows to conclude for the global asymptotic stability of the origin of the state space for system (A.5), and thus of the equilibrium point for the overall closed loop system (A.4), (A.5).

ACKNOWLEDGEMENTS

This work was done while Paolo Rocco was a visiting scholar at the George W. Woodruff School of Mechanical Engineering of the Georgia Institute of Technology, sponsored by the Italian National Research Council (CNR) under NATO Grant No. 215.27/11-216.1865.

REFERENCES

[1] Book, W. J. (1993), "Controlled Motion in an Elastic World", *ASME Journ. of Dyn. Syst., Meas. and Control,* Vol. **115**, pp. 252-261.

[2] Book, W. J. (1984), "Recursive Lagrangian Dynamics of Flexible Manipulator Arms", *The Int. Journ. of Rob. Res.*, Vol. **3**, pp. 87-101.

[3] Cetinkunt, S. and W. J. Book (1989), "Symbolic Modeling and Dynamic Simulation of Robotic Manipulators with Compliant Links and Joints", *Robotics and Comp.-Integr. Manufact.*, Vol. **5**, pp. 301-310.

[4] Magee, D. P. and W. J. Book (1993), "Control and Control Theory for Flexible Robots", *Journ. SICE,* Vol. **32**, pp. 309-317.

[5] Spong, M. W. (1987), "Modelling and Control of Elastic Joint Robots", *ASME Journ. of Dyn. Syst., Meas. and Control,* Vol. **109**, pp. 310-319.

[6] Wang, D. and M. Vidyasagar, (1989), "Feedback Linearizability of Multi-Link Manipulators with One Flexible Link", *Proc. IEEE Conf. Dec. Contr.*, pp. 2072-2077.

[7] Siciliano, B. and W. J. Book (1988), "A Singular Perturbation Approach to Control of Lightweight Flexible Manipulators", *Int. Journ. of Rob. Res.*, Vol. **7**, pp. 79-90.

[8] Siciliano, B., J. V. R. Prasad and A. J. Calise (1992), "Output Feedback Two-Time Scale Control of Multilink Flexible Arms", *ASME Journ. of Dyn. Syst., Meas. and Control,* Vol. **114**, pp. 70-77.

[9] Kokotovic, P., H. K. Khalil and J. O'Reilly (1986), *"Singular Perturbation Methods in Control: Analysis and Design"*, Academic Press.

[10] Vukobratovich, M. and D. Surdilovic (1993), "Control of Robotic Systems in Contact Tasks: an Overview", in: *Tutorial on Force and Contact Control in robotic systems, IEEE Int. Conf. on Rob. and Aut.*, pp. 13-32.

[11] Eppinger, S. D. and W. P. Seering (1988), "Modeling Robot Flexibility for Endpoint Force Control", *Proc. IEEE Int. Conf. on Rob. and Autom.*, pp. 165-170.

[12] Li, D. (1990), "Tip-contact Force Control of One-link Flexible Manipulator: an Inherent Performance Limitation", *Proc. Amer. Contr. Conf.*, pp. 697-701.

[13] Chiou, B. C. and M. Shahinpoor (1988), "Dynamic Stability Analysis of a One-Link Force-Controlled Flexible Manipulator", *Journ. of Rob. Syst..*, Vol. **5**, pp. 443-451.

[14] Chiou, B. C. and M. Shahinpoor (1990), "Dynamic Stability Analysis of a Two-Link Force-Controlled Flexible Manipulator", *ASME Journ. of Dyn. Systems, Measur. and Control.*, Vol. **112**, pp. 661-666.

[15] Yim, W. and S. N. Singh (1993), "Inverse Force/End-Point Control, Zero Dynamics and Stabilization of Constrained Elastic Robots", *Proc. Amer. Contr. Conf.*, pp. 2873-2878.

[16] Yim, W. and S. N. Singh (1994), "Sliding Mode Force and Motion Control and Stabilization of Elastic Manipulator in the Presence of Uncertainties", *Proc. IEEE Int. Conf. on Rob. and Autom.*, pp. 2113-2118.

[17] Lew, J. Y. and W. J. Book (1993), "Hybrid Control of Flexible Manipulators with Multiple Contacts", *Proc. IEEE Int. Conf. on Rob. and Autom.*, pp. 242-247.

[18] Yoshikawa T., K. Hosoda, K. Harada, A. Matsumoto and H. Murakami (1994), "Hybrid Position/Force Control of Flexible Manipulators by Macro-Micro Manipulator System", *Proc. IEEE Int. Conf. on Rob. and Autom.*, pp. 2125-2130.

[19] Matsuno, F., T. Asano and Y. Sakawa (1994), "Modeling and Quasi-Static Hybrid Position/Force Control of Constrained Planar Two-Link Flexible Manipulators", *IEEE Trans. on Rob. and Autom.*, Vol. **10**, pp. 287-297.

[20] Matsuno, F. and K. Yamamoto (1993), "Dynamic Hybrid Position/force Control of a Flexible Manipulator", *Proc. IEEE Int. Conf. on Rob. and Autom.*, pp. 462-467.

[21] Mills, J. K. (1992), "Stability and Control Aspects of Flexible Link Robot Manipulators During Constrained Motion Tasks", *Journ. of Rob. Syst.*, Vol. **9**, pp. 933-953.

[22] Yang, J., F. Lian and L. Fu (1995), "Adaptive Hybrid Position/Force Control for Robotic Manipulators with

Compliant Links", *Proc. IEEE Int. Conf. on Rob. and Autom.*, pp. 603-608.
[23] Hu, F. L. and A. G. Ulsoy (1994), "Force and Motion Control of a Constrained Flexible Arm", *ASME Journ. of Dyn. Systems, Measur. and Control.*, Vol. **116**, pp. 336-343.
[24] Ferretti, G., G. Magnani and P. Rocco (1995), "Towards the Implementation of Hybrid Position/Force Control in Industrial Robots", submitted to *IEEE Trans. on Rob. and Aut.*
[25] Rocco, P. (1995), "Force/Position Control Algorithms for Industrial Robots: Theoretical Analysis and Implementation (in Italian)", *PhD Dissertation,* Politecnico di Milano, Italy.
[26] Meirovitch, L. (1986), "*Elements of Vibration Analysis*", McGraw-Hill.
[27] Wehage, R. A. and E. J. Haug (1982), "Generalized Coordinate Partitioning for Dimension Reduction in Analysis of Constrained Dynamic Systems", *ASME Journ. of Mech. Design*, Vol. **104**, pp. 247-255.
[28] McClamroch, N. H. and D. Wang (1988), "Feedback Stabilization and Tracking of Constrained Robots", *IEEE Trans. on Aut. Contr.*, Vol. **33**, pp. 419-426.
[29] Jankowski, K. P. and H. A. ElMaraghy (1992), "Dynamic Decoupling for Hybrid Control of Rigid-/Flexible-Joint Robots Interacting with the Environment", *IEEE Trans. on Rob. and Aut.*, Vol. **8**, pp. 519-534.
[30] Mills, J. K. (1992b), "Stability and Control of Elastic-Joint Robotic Manipulators During Constrained-Motion Tasks", *IEEE Trans. on Rob. and Aut.*, Vol. **8**, pp. 119-126.
[31] Ferretti, G., C. Maffezzoni, G. Magnani and P. Rocco (1993), "Decoupling Force and Motion Control in Industrail Robots", *Contr. Eng. Practice*, Vol. **1**, pp. 1019-1027.
[32] Takegaki, M. and S. Arimoto, (1981), "A New Feedback Method for Dynamic Control of Manipulators", *ASME Journ. of Dyn. Syst., Meas. and Control*, Vol. **103**, pp. 119-125.
[33] Kwon, D. S. and W. J. Book (1994), "A Time-Domain Inverse Dynamic Tracking Control of a Single-Link Flexible Manipulator", *ASME Journ. of Dyn. Systems, Measur. and Control.*, Vol. **116**, pp. 193-200.
[34] Grace, A., A. J. Laub, J. N. Little and C. Thompson (1990), "*Control System Toolbox For Use With Matlab*", The MathWorks.
[35] Spong, M. W. and M. Vidyasagar (1989), "*Robot Dynamics and Control*", John Wiley & Sons.

Captions for figures

Fig.1: Sketch of the force controller

Fig. 2: The experimental arm RALF

Fig. 3: Simulation plant

Fig. 4: Maximum real part of the closed loop eigenvalues for the fast system

Fig 5: Force response with slow and fast control

Fig 6: Force response with only slow control

Fig 7: Force history during trajectory tracking

Fig 8: Trajectory tracking error

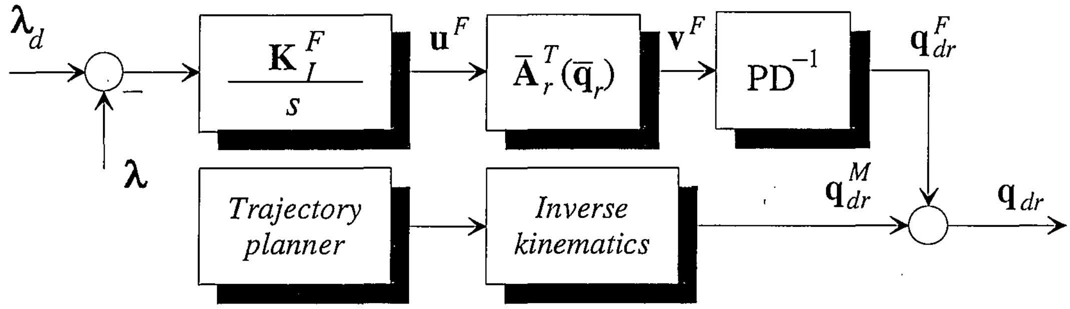
λ_d
λ
$\frac{K_I^F}{s}$
u^F
$\bar{A}_r^T(\bar{q}_r)$
v^F
PD^{-1}
q_{dr}^F
Trajectory planner
Inverse kinematics
q_{dr}^M
q_{dr}

Fig. 1

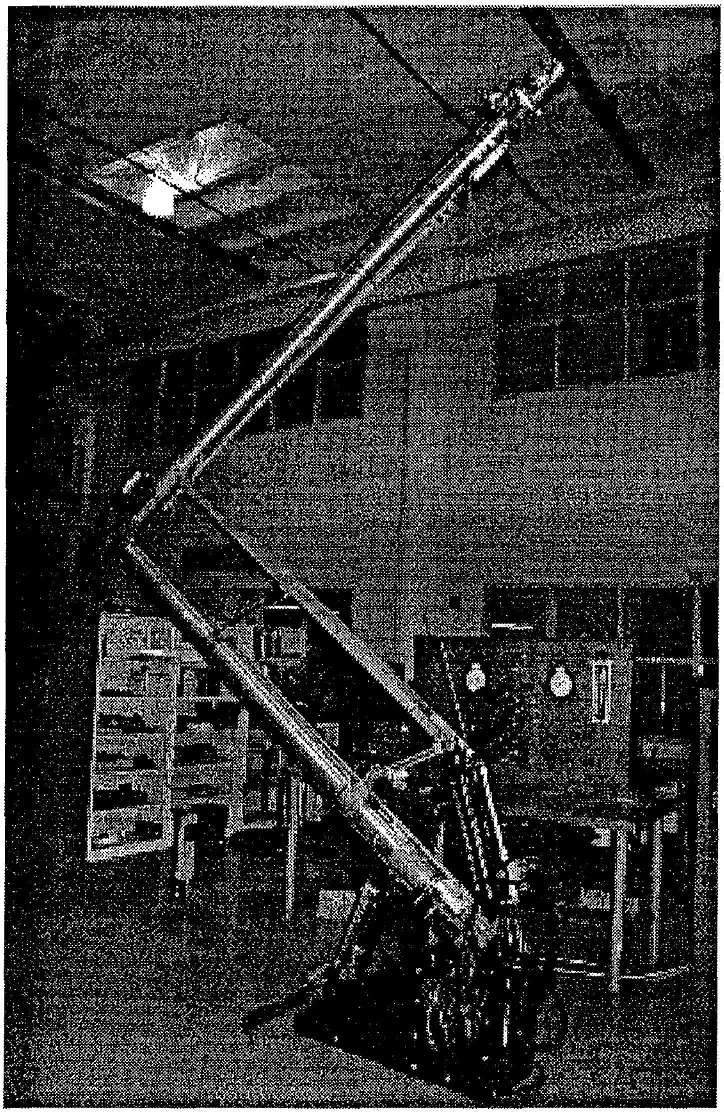

Fig. 2

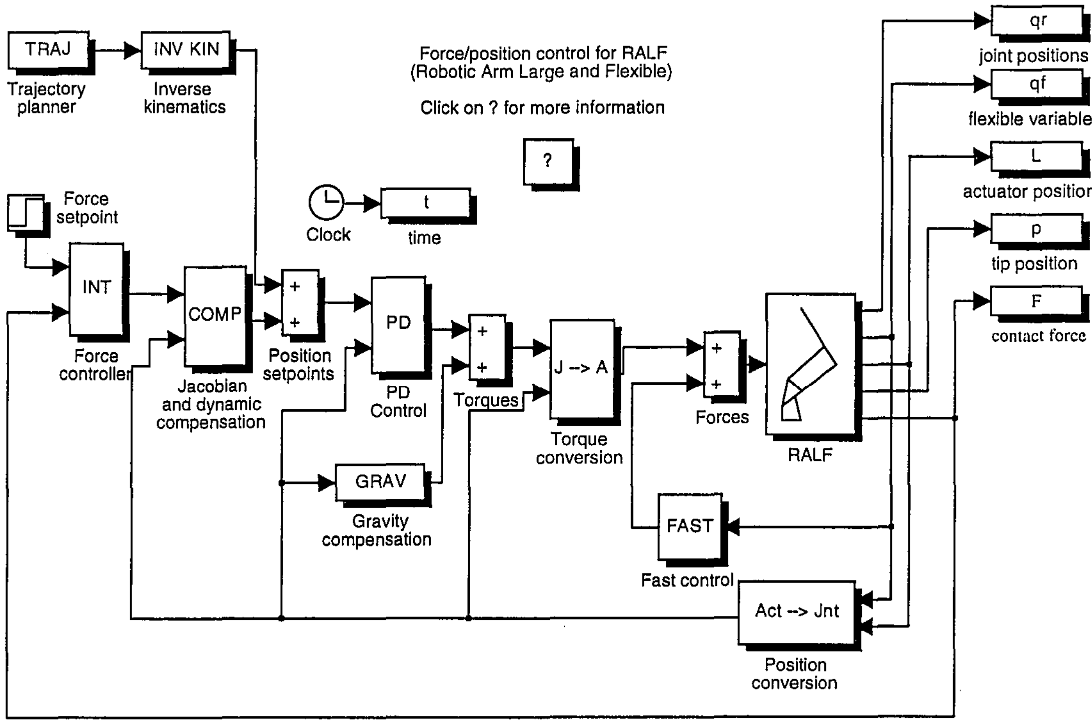
Force/position control for RALF
(Robotic Arm Large and Flexible)
Click on ? for more information
?
TRAJ
Trajectory planner
INV KIN
Inverse kinematics
Force setpoint
Clock
t
time
INT
Force controller
COMP
Jacobian and dynamic compensation
+
+
Position setpoints
PD
PD Control
+
+
Torques
GRAV
Gravity compensation
J --> A
Torque conversion
+
+
Forces
RALF
FAST
Fast control
Act --> Jnt
Position conversion
qr
joint positions
qf
flexible variables
L
actuator positions
p
tip position
F
contact force

Fig. 3

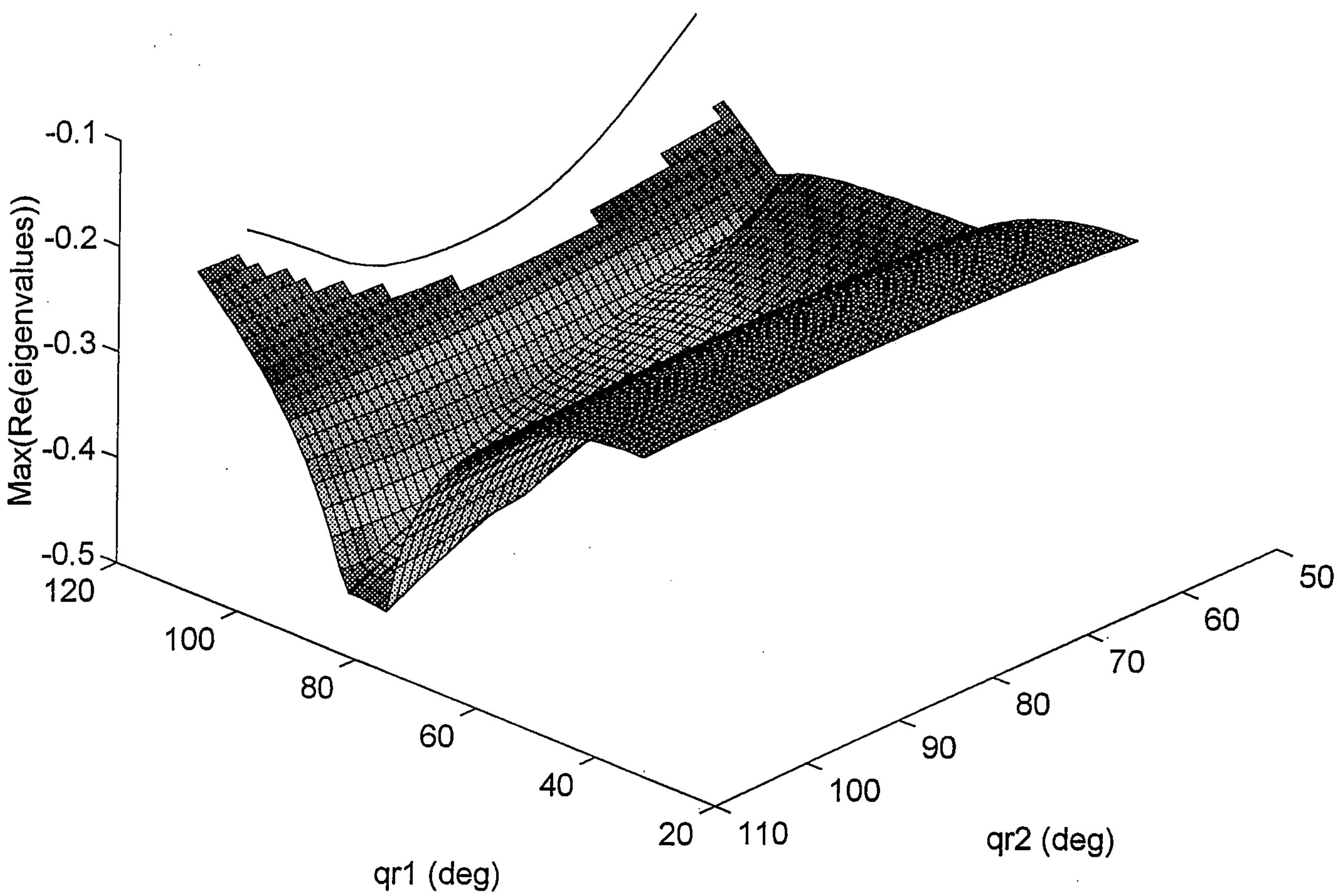

-0.1
-0.2
-0.3
-0.4
-0.5
Max(Re(eigenvalues))
120
100
80
60
40
20
qr1 (deg)
110
100
90
80
70
60
50
qr2 (deg)

Fig. 4

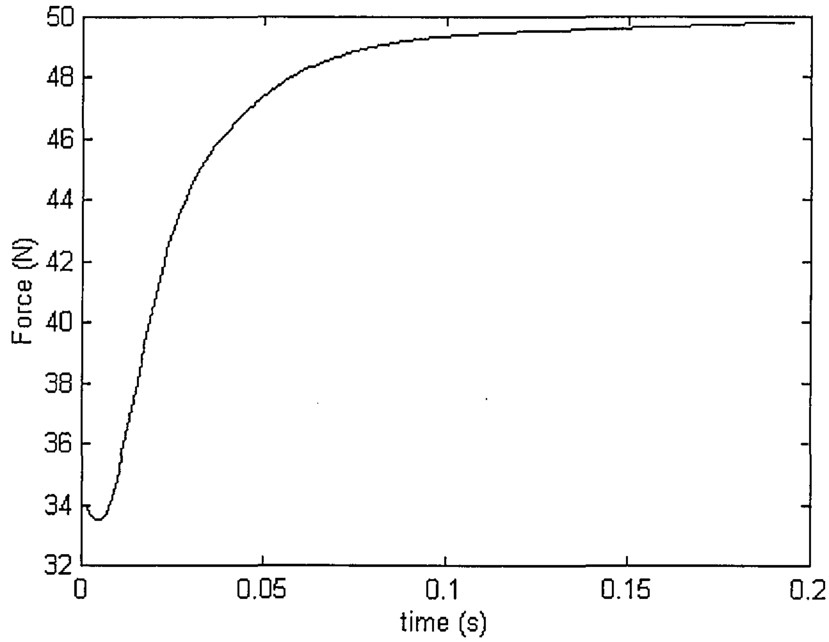

Fig. 5

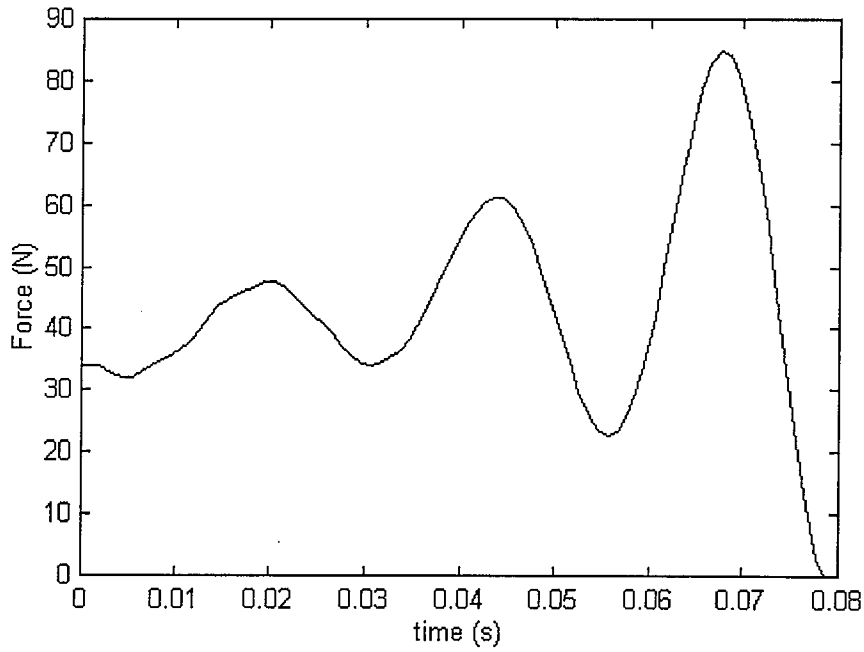

Force (N)
time (s)
0
10
20
30
40
50
60
70
80
90
0
0.01
0.02
0.03
0.04
0.05
0.06
0.07
0.08

Fig. 6

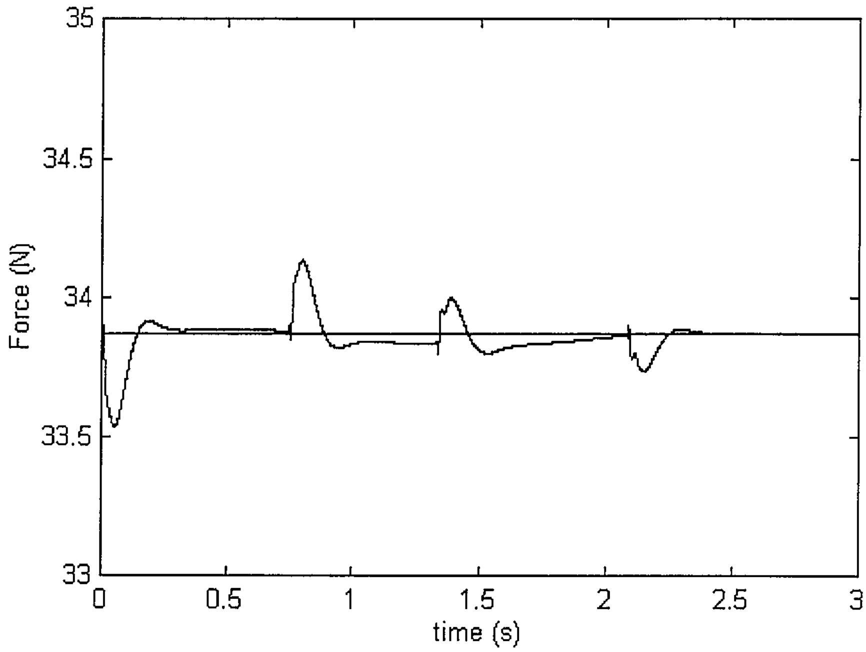

Fig. 7

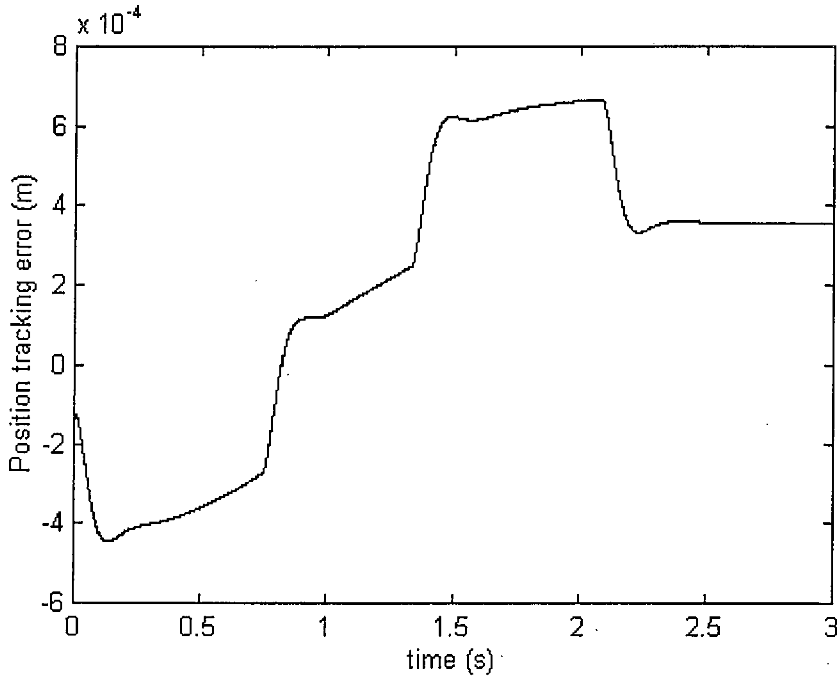

Fig. 8